

Recreating the hematoma: microfabrication of artificial haematopoietic stem cell microniche *in vitro* using dielectrophoresis

Gerard H. Markx · Louise Carney · Mike Littlefair · Anil Sebastian · Anne-Marie Buckle

© Springer Science + Business Media, LLC 2008

Abstract The hematoma is a three-dimensional aggregate of cells which is able to produce all blood types. To be able to do this, it must be able to create within the cell aggregate a microenvironment which enables haematopoietic stem cell maintenance, renewal and differentiation. A first step was taken towards the creation of artificial haematopoietic stem cell microniche *in vitro* by the creation with dielectrophoresis of hemispherical cell aggregates of a height of 50–100 μm with a defined internal architecture similar to that of a putative hematoma. It is shown that, after their dielectrophoretic manipulation, the cells remain viable and active. Cells within the aggregate are in direct contact with

each other, potentially allowing direct cell–cell communication within the cell construct. Some cell immobilisation methods are explored for further stabilising the 3-D organisation of the cell aggregate after its formation. The introduction of traceable individual cells into the artificial microniche is demonstrated.

Keywords Dielectrophoresis · Microenvironment · 3-D cell culture · Microniche · Haematopoiesis · Stem cell

1 Background

Blood formation (haemopoiesis or haematopoiesis; Zon 2001) in mammals mainly takes place in the extravascular spaces between marrow sinuses, where the haematopoietic cells lie in cords or wedges (Abboud and Lichtman 2001). Stem cell development in the marrow sinuses requires the support of stromal cells, and it has been proposed that stromal cells and haematopoietic precursors form specific units under physiological conditions (Blazsek et al. 1988). On this basis a multicellular functional unit of haematopoiesis has been defined, and termed a hematoma (Blazsek et al. 1990).

Studies on the particulate fraction of bone marrow aspirates have shown that the multicellular material within the isolates comprised the most active and productive part of bone marrow (Blazsek et al. 1988, 1990, 1999), rather than the buffy coat fraction, which mainly contains single cells. This has led to the proposal that multicellular spheroids isolated from bone marrow are hematoma units. Subsequent studies of the spheroids (Blazsek et al. 1988) revealed that they are structurally organised, with a predominance of adipocytes and preadipocytes, osteogenic mesenchymal cells, reticulocytes and macrophages in the core, and

G. H. Markx
Department of Chemical Engineering,
School of Engineering and Physical Sciences,
Heriot-Watt University,
Riccarton, Edinburgh, Scotland, UK

L. Carney · M. Littlefair · A. Sebastian
School of Chemical Engineering and Analytical Science,
Manchester Interdisciplinary Biocentre,
The University of Manchester,
Manchester, UK

A.-M. Buckle
Faculty of Life Sciences, Manchester Interdisciplinary Biocentre,
The University of Manchester,
Manchester, UK

G. H. Markx (✉)
Microstructures and Microenvironment Research Group,
Department of Chemical Engineering,
School of Engineering and Physical Sciences,
Heriot-Watt University,
Riccarton, Edinburgh, Scotland, UK
e-mail: g.h.markx@hw.ac.uk

myeloid, erythroid, and megakaryocytic progenitor cells and their progeny at the periphery (Blazsek et al. 1990). The most recent data on the hematopoietic stem cell activity (Blazsek et al. 2000) has confirmed that haematopoietic stem cell activity is highly enriched in hematopoietic niches, indicating that stromal cells in the hematopoietic niche specifically control the growth and development of stem cells. Furthermore it has been proposed (Blazsek et al. 2000) that these specialised niches are limited in number, thereby regulating stem cell activity through saturation of the stem cell niche.

Fluctuations in demand for mature cells in adult blood require control of stem cell activity by extrinsic factors produced within the local stem cell niche. As mature cells leave the marrow niches are vacated, and as different microniches become available, the differentiation process will take niche specific differentiation routes. The microniches available for the cells are in turn determined by the spatial organisation and composition of a cell's surroundings and the interaction with other cells, either through direct cell–cell contact mediated by integral membrane proteins or through secreted factors (Watt and Hogan 2000). Control over the microniches available for cells could enable one to control a cell's physiology, differentiation and development.

Although the concept of the stem cell niche originated in the study of haematopoietic stem cells (HSC) in *in vitro* cultures, current culture systems do not comprise a good representation of bone marrow *in vivo*. Current culture systems make use of stromal monolayers overlaid with HSCs which, after several weeks, give rise to areas of active stem cell proliferation and differentiation (cobblestone areas, CA), the presence of which are the most reliable indicator of stem cell activity *in vitro* to date. However, such systems do not take into account the three-dimensional nature of the *in vivo* stem cell microenvironment. Thus, our understanding of the haematopoietic stem cell microenvironment could be much improved if we studied 3-D systems rather than 2-D systems.

The assembly of three-dimensional multicellular structures from component cells is a topic which is at the heart of tissue engineering. A wide variety of approaches have previously been used (Bhatia 1999; Tsang and Bhatia 2004). Methods used for the construction of three-dimensional artificial tissues include the assembly of layers of cultured cells sheets (Shimizu et al. 2003), printing of cell aggregates (Burg and Boland 2003; Mironov et al. 2003) and guidance of cells by physical techniques such as optical trapping (Odde and Renn 2000), ultrasound (Haake et al. 2005a, b; Haake and Dual 2004), magnetic (Ito et al. 2004) and electrical (Albrecht et al. 2006; Alp et al. 2003; Ho et al. 2006; Sebastian et al. 2006, 2007) forces, the formation of gels entrapping cells in microfluidic molds (Tan and Desai 2004) and photopatterning of cell-laden hydrogels (Liu and Bhatia 2002). To

date these techniques have mainly been used in proof-of-principle experiments, and to make relatively simple mammalian tissues. Also, the tissues made have been relatively static. Bone marrow, in contrast, is a highly dynamic system designed to respond rapidly to fluctuations in demand for cells.

In this paper we will describe one possible method of controlling microniches, which is based on the creation of aggregates with three-dimensional organisation using positive dielectrophoresis, i.e. the movement of particles in non-uniform electric fields towards high field regions (Albrecht et al. 2006; Alp et al. 2003; Ho et al. 2006; Hughes 2002; Jones 1995; Morgan and Green 2001; Sebastian et al. 2006, 2007). The dielectrophoretic method forms a technique which allows the creation of three-dimensional cell aggregates with defined architectures, at low cost, with relatively simple equipment. The utility of this technique had previously been demonstrated in experiments involving the formation of three-dimensional aggregates of microbial cells with defined internal architectures (Alp et al. 2002; Andrews et al. 2006; Mason et al. 2005; Verduzco-Luque et al. 2003). The technique developed involves guiding cells by dielectrophoresis to high electric field regions between microelectrodes, and subsequently immobilising them (Alp et al. 2002; Verduzco-Luque et al. 2003). Recent work has allowed us to adapt this approach and use it with mammalian cells (Alp et al. 2003; Sebastian et al. 2006, 2007). We will now show that the technology can be used to construct artificial three dimensional microenvironments for haematopoietic stem cells.

2 Experimental details

2.1 Materials and methods

2.1.1 Cells

Jurkat cells (human T lymphocytes) were seeded at a concentration of 5×10^4 cells per milliliter in RPMI 1640 medium supplemented with 10% fetal calf serum (FCS), 2 mM glutamine, 100 U ml⁻¹ penicillin and 100 µg ml⁻¹ streptomycin. Cells were cultured in a humidified chamber with 5% CO₂ at 37°C for 40–48 h, and then harvested by centrifugation at 1,600 rpm for 5 min.

Mouse AC3 stromal cells were seeded at a concentration of 1×10^4 per 25 cm² of flask growth area in RPMI 1640 medium supplemented with 5% FCS, 1 µg ml⁻¹ β-mercaptoethanol, 10 µg ml⁻¹ sodium pyruvate, 12 mM glutamine, 100 U ml⁻¹ penicillin and 100 µg ml⁻¹ streptomycin. The stromal cells were grown adherently in a humidified chamber with 5% CO₂ at 37°C until near 100%

confluence was obtained after 8–10 days. Medium was exchanged every 3 days. Prior to cell harvesting, the cells were suspended using filter sterilized 0.5% trypsin and 0.5% ethylene diamine tetra acetic acid (EDTA) dissolved in $1\times$ PBS. Cells were then harvested by centrifugation at 1,600 rpm for 5 min.

SAOS-2 osteoblast cells were seeded at a concentration of 1×10^4 cell per 25 cm^2 of flask growth area in McCoy's 5A modified medium supplemented with 15% FCS, 12 mM glutamine, 100 U ml^{-1} penicillin and $100\text{ }\mu\text{g ml}^{-1}$ streptomycin in a humidified chamber with 5% CO_2 at 37°C . Medium was exchanged every 3 days. The cells reached 100% confluence in 8–10 days. The cells were harvested by centrifugation (1,600 rpm, 5 min) using filter sterilized 0.5% trypsin and 0.5% ethylene diamine tetra acetic acid (EDTA) dissolved in $1\times$ PBS.

Prior to their use in dielectrophoretic experiments, harvested cells were washed twice by centrifugation at 1,600 rpm for 4 min with 480 mM D-sorbitol. The cells were then resuspended in 480 mM D-sorbitol solution at a concentration of 5×10^5 cells per milliliter.

In some experiments cells were fluorescently stained in order to facilitate their distinction. Jurkat cells were stained with the red fluorescent PKH26 membrane stain (Sigma), whilst AC3 cells were stained with the green fluorescent PKH2 membrane stain (Sigma). The concentrations of PKH26 and PKH2 stains were 8×10^{-6} and 4×10^{-6} M respectively for 1×10^7 cells per milliliter. After staining the cells were washed with 480 mM D-sorbitol twice, and then resuspended in 480 mM D-sorbitol. Osteoblast cells (SAOS-2) were suspended in RPMI medium, and Draq 5 nuclear stain was introduced at a final concentration of $10\text{ }\mu\text{M}$. After incubating the cells for 5 min they were washed with growth medium followed by washing (twice) and resuspension in 480 mM sorbitol. The Draq 5 stain fluoresces in the far red region, but a cyan colour was assigned to the stain during post-processing after confocal microscopy.

2.1.2 Cell viability

Propidium iodide was used in order to determine cell viability during exposure to the electrical field. The propidium iodide was added to the cells at a concentration of $5\text{ }\mu\text{g ml}^{-1}$ immediately after the washing stage. Dead cells could be identified because they fluoresced red, whilst live cells remained unstained.

Experiments were performed with cells suspended in 480 mM D-sorbitol. Although this is higher than physiological osmotic strength (300 mM), no deleterious effects on the cell viability were observed. Currently all experiments with mammalian cells in our group are performed with 300 mM D-sorbitol.

2.1.3 Microelectrodes

The microelectrodes were made by photolithography as described previously (Flores-Rodriguez and Markx 2006). For all experiments, indium tin oxide (ITO) microelectrodes of the interdigitated oppositely castellated design were used with characteristic sizes between 50 and $250\text{ }\mu\text{m}$ (Venkatesh and Markx 2006). Chambers with a height of $500\text{ }\mu\text{m}$ were made on top of the electrodes using a silicone spacer (Grace Biolabs) and a microscope slide cover slip. When necessary, needles connected to silicone tubing were placed under the cover slip to allow the fluid in the chamber to be introduced or replaced.

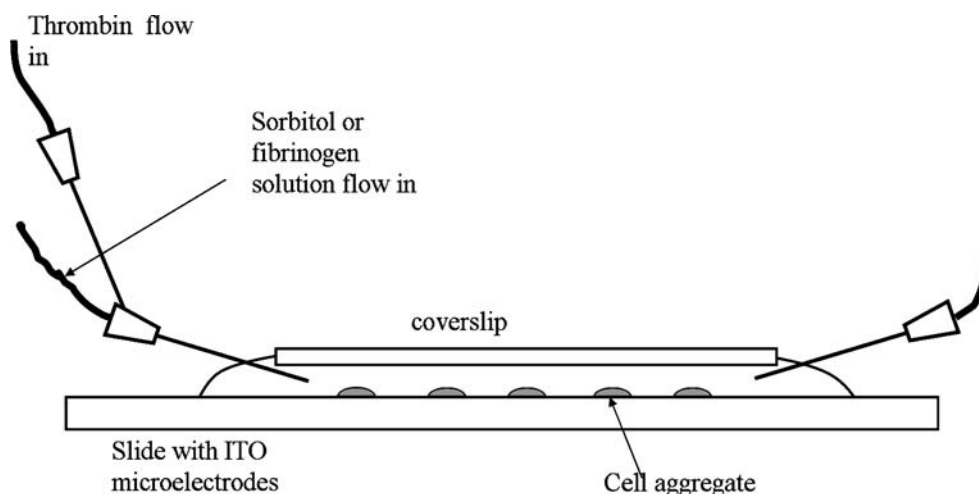
2.1.4 Formation of cell aggregates

The chamber was filled with a low conductivity D-sorbitol solution prior to the application of any electric current. Electric fields of 1 MHz frequency were generated using a Thurlby–Thandar TG120 function generator using voltages up to $20\text{ V}_{\text{pk-pk}}$. Cells were introduced into the chamber with a Gilson Minipuls 3 pump at a concentration of 5×10^5 cells per milliliter and attracted to the high field regions between the castellations. A continuous small flow of fresh sorbitol solution was maintained in the chamber in order to redistribute the cells, remove non-attracted cells and keep the medium conductivity around the cells low. Cells were added until the aggregate reached the desired height, or the height stopped increasing. This was usually achieved after a few minutes, and a maximum of 15 min.

A Nikon E600 microscope equipped with a Nikon Coolpix 4500 digital camera was used to observe the aggregates during their formation. Aggregate heights were measured as described previously (Sebastian et al. 2006; Venkatesh and Markx 2006) by consecutively focusing on the electrode plane or on the top of the aggregate. Aggregate height could be determined from the scales on the fine focus control of the microscope. Where information on the three-dimensional structure of the aggregates was needed, a Zeiss LSM 500 confocal microscope was used. Images were analyzed using Zeiss LSM image browser and SigmaScan-Pro 5.0, Systat.

In order to form layered aggregates, cells which were to form the bottom layer were first introduced into the chamber and attracted to the high field regions between the castellations with positive dielectrophoresis using a signal of 1 MHz, $20\text{ V}_{\text{pk-pk}}$. Cells were added until the aggregation of the cells had acquired the required height. Following this, cells of another cell type were introduced and layered on top of the previous cells until the required layer thickness was achieved. In some experiments a third cell type was deposited on top of the previous two cell

Fig. 1 Schematic drawing of setup used to immobilise cells in fibrin gel



layers in order to form aggregates with layers of three different cell types.

2.1.5 Cell immobilization

A fibrin gel was used to immobilise the cells in the aggregate. A solution of 10 mg ml^{-1} of bovine fibrinogen was prepared in growth medium (RPMI-1640), and a solution of 10 U of bovine thrombin was prepared in $4 \text{ }\mu\text{M}$ calcium chloride solution. Both solutions were filter sterilized. The chamber was autoclaved prior to this to ensure sterility. Jurkat or osteoblast cells were aggregated with dielectrophoresis ($20 \text{ V}_{\text{pk-pk}}$, 1 MHz) between the castellations of electrodes with a characteristic size of $200 \text{ }\mu\text{m}$, under a continuous flow of 480 mM D-sorbitol. The electric field was then maintained

for a further 10–15 min, in order to induce adhesion between the cells (Sebastian et al. 2007). Following this, the thrombin solution was pumped through a hole in the side of a needle into another needle at a rate of $2.7 \text{ }\mu\text{l min}^{-1}$ and mixed with a flow of $25 \text{ }\mu\text{l min}^{-1}$ of fibrinogen dissolved in growth medium. The mixture was then introduced into the chamber formed by a coverslip covering the electrodes (see Fig. 1). The superficial velocity of the mixture through the chamber was $5.5 \text{ }\mu\text{m s}^{-1}$. When the chamber was completely filled with the immobilisation mixture the flow was stopped. The formation of the fibrin gel occurred within 10 min from the start of the flow. When the gel had formed the cover slip was carefully removed using a surgical blade, and the slide with the immobilised aggregates was then transferred to a sterile petri dish and cell growth medium was added. The

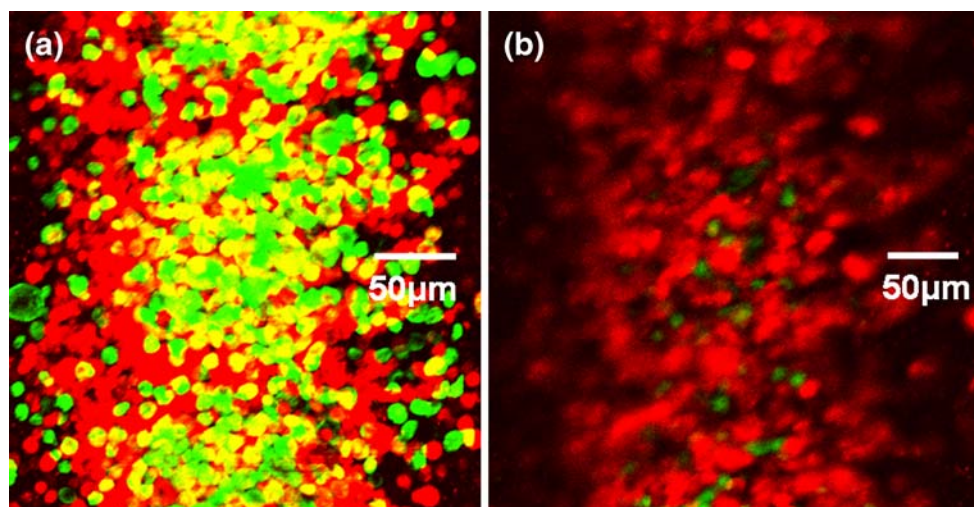
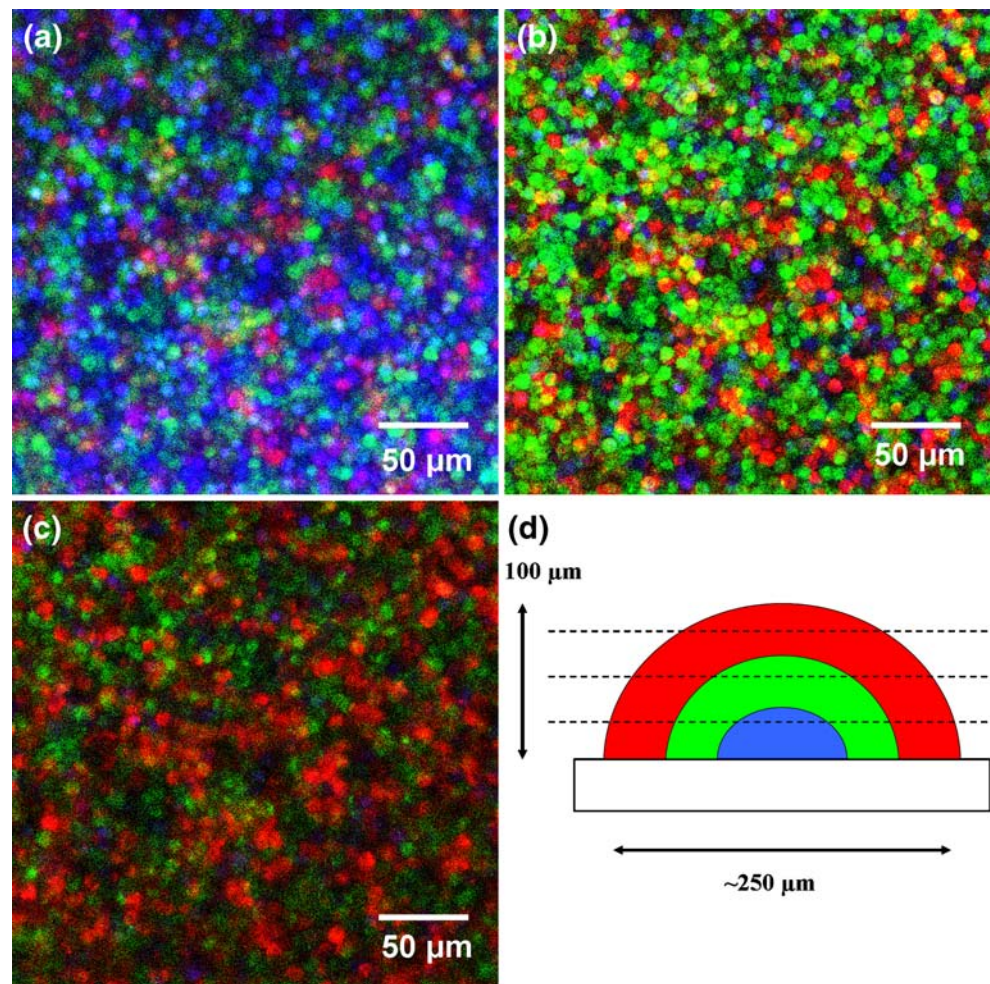


Fig. 2 Confocal microscopy sections of aggregates of stromal AC3 cells (stained green) covered by Jurkat cells (stained red), formed by positive dielectrophoresis (1 MHz, $10 \text{ V}_{\text{pk-pk}}$) at interdigitated oppositely castellated electrodes with a characteristic size of $100 \text{ }\mu\text{m}$. (a) Section through aggregate at a height of $52 \text{ }\mu\text{m}$; (b) idem, at a height

of $72 \text{ }\mu\text{m}$. The total height of the aggregate was $78 \text{ }\mu\text{m}$. The section through the bottom of the aggregate at (a) clearly shows the centre core of the aggregates is formed by the green fluorescent stromal cells, whilst the section at (b) through a higher part of the aggregate shows predominantly the red fluorescent Jurkat cells

Fig. 3 Confocal images of three-layered aggregate, created using dielectrophoresis at $20 V_{pk-pk}$, 1 MHz, at electrodes with a characteristic size of $200 \mu m$. **(a)** section through the bottom layer at $16 \mu m$ above the electrode plane, showing the osteoblast cells stained with Draq5; although the cells fluorescence in the far red, cyan was assigned as a false colour; **(b)** section through the middle layer at $56 \mu m$ above the electrode plane, showing the predominance of stromal cells stained green with PKH2; **(c)** section through the top layer at $80 \mu m$ above the electrode plane, showing predominantly Jurkat cells stained red with PKH26. **(d)** Schematic outline of aggregate; the dashed lines correspond to confocal microscopy images **(a–c)**



aggregates were microscopically investigated every day for up to 6 days after their formation.

3 Results and discussion

3.1 Formation of hematoin-like structures

The hematoin consists of at least two distinct structures, i.e. an inner core of mainly support cells and an outer layer of mainly blood producing cells. To mimic the hematoin structure, aggregates were first made with dielectrophoresis consisting of an inner core of stromal cells, surrounded by an outer layer of Jurkat T-lymphocytes. The stromal cells were stained with a green fluorescent dye, and the Jurkat cells with a red fluorescent dye, and confocal microscopy was used to investigate the distribution of cells within the hematoin-like aggregates.

Procedures for creating multilayered aggregates of mammalian cells were published before (Sebastian et al. 2006). In this case, aggregates of Jurkat cells on top of stromal cells were made at electrodes of the interdigitated oppositely

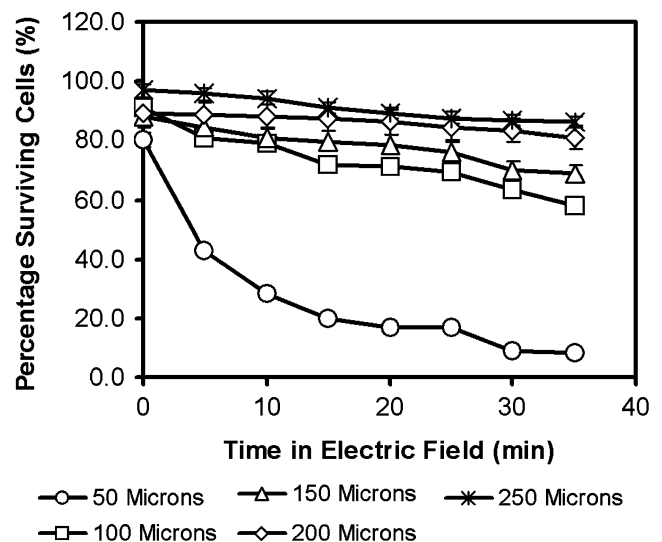


Fig. 4 Percentage of surviving Jurkat cells during continuous exposure to a signal of 1 MHz, $10 V_{pk-pk}$ after the formation of aggregates by positive dielectrophoresis between oppositely castellated electrodes of different characteristics sizes. During the experiment the cells were continuously immersed in a 480-mM sorbitol solution with 1×10^{-5} M propidiumiodide

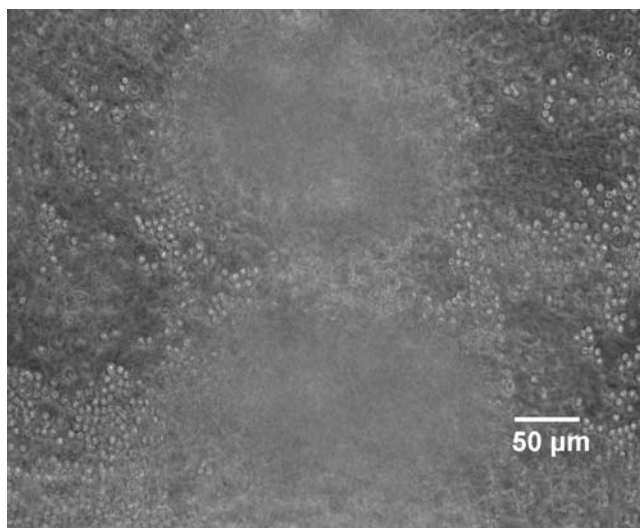


Fig. 5 Aggregates of Jurkat cells formed at electrodes of 200 μm characteristic size after their immobilisation in a fibrin gel made by the polymerisation of fibrinogen using thrombin

castellated design by applying a signal of 20 $V_{\text{pk-pk}}$, 1 MHz to electrodes with a characteristic size of 200 μm .

Figure 2 shows confocal microscopy sections through layers at two different heights in the artificial hematon-like structure, clearly showing that the green fluorescent stromal cells dominate the lower layer, and the Jurkat cells the upper layer.

3.2 Formation of three-layered aggregates

Whilst stromal cells are essential in maintaining the viability of haematopoietic stem cells due to their production of essential growth factors, cytokines and other signals, osteoblasts have been shown to be essential in maintaining the hematopoietic stem cells' stemcellness (Calvi et al.

2003). Thus, any attempt to recreate the microenvironment of haematopoietic stem cells should include osteoblast or osteoblast-like cells.

Aggregates with three different layers of cells, i.e. osteoblasts, covered by stromal cells, which in turn are covered by Jurkat cells, are shown in Fig. 3.

3.3 Effect of the electrical field on cell viability

The viability of Jurkat cells during electric field exposure was followed to find out whether the electric field had a negative effect on the cells (Archer et al. 1999; Menachery and Pethig 2005). Cells were taken from the flask, centrifuged, the pellet washed twice with 480 mM sorbitol, and then resuspended in a sorbitol solution which also contained 1×10^{-5} M propidium iodide. Aggregates were made of the cells at electrodes of different sizes using a signal of 10 $V_{\text{pk-pk}}$, 1 MHz, and after the formation of the aggregates the uptake of the fluorescent stain by the cells was followed. Cells whose viability was impaired would stain red. The results are presented in Fig. 4, and confirm previous experiments (Sebastian et al. 2007) indicating that cell death caused by electric field exposure will be limited to below 10% for the conditions used in our experiments.

3.4 Immobilization of cells in fibrin

It was previously found that, when aggregates were formed in a low conductivity 480 mM sorbitol buffer and the cell were exposed to the electric field for a further 10–15 min after the aggregate had fully formed, the cells adhered strongly to each other (Sebastian et al. 2007). Replacement of the D-sorbitol solution by growth medium (RPMI 1640) was not only possible, but actually increased the strength of the aggregates (Sebastian et al. 2007), arguably by

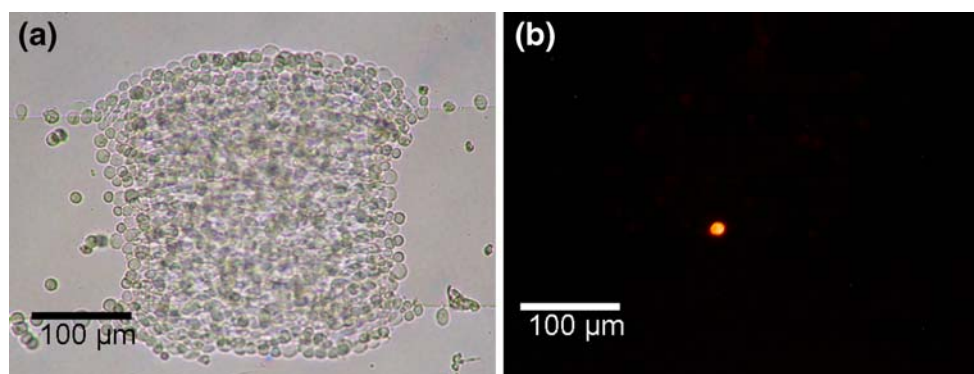


Fig. 6 Introduction of a stem cell in a hematon-like structure. (a) Brightfield image of an aggregate formed with Jurkat cells using dielectrophoresis at 1 MHz, 10 $V_{\text{pk-pk}}$ at microelectrodes of 200 μm characteristic size. Following the construction of the aggregates a stem cell was introduced which was stained with PKH26. (b) Fluorescent

image of the same aggregate. The bright red/orange cell is the stem cell. Hematon-like bilayer structures with AC3 stromal cells/Jurkat cells, and three-layered structures with AC3 stromal, osteoblast and Jurkat cells were obtained using a similar method

crosslinking of the cells by divalent ions such as Ca^{2+} and Mg^{2+} present in the medium. The method was used with both Jurkat cells and osteoblasts, and stable aggregates could be produced of both cell types using this method. Upon incubation of the aggregates, however, it was found that after 24 h considerable cell movement had occurred. In the case of Jurkat cells (which normally grow in suspension) the cells had reverted to type, i.e. the aggregates had disappeared, and the Jurkat cells were again growing in suspension as single cells or in loose aggregates. In the case of osteoblasts (which grow adherently) after 24 h the aggregate height had significantly reduced (from approximately 100 μm to approximately 20 μm) as the cells in the aggregate had started to spread over the surface. It was therefore deemed necessary to explore gel immobilisation to keep the cells in place once the aggregates had formed.

Aggregates of Jurkat or osteoblast cells were formed with dielectrophoresis at 1 MHz, 20 $V_{\text{pk-pk}}$ at microelectrodes of 200 μm characteristic size, and the electric field was maintained for a further 15 min to allow the cells to adhere to each other. The adhesive forces between the cells were then strong enough to allow the sorbitol buffer to be replaced by RPMI 1640 medium. The RPMI 1640 flow was then replaced by a 10:1 mixture of RPMI 1640 medium containing fibrinogen (10 mg ml^{-1}) and a 4 μM CaCl_2 solution containing 10 U of thrombin per milliliter. A fibrin gel was formed after approximately 10 min, effectively immobilising the cells (see Fig. 5).

Microscopic observation of the aggregates for 6 days showed some but very limited spreading of the cells from the aggregate. Also, the aggregates maintained their height.

3.5 Introduction of stem cells into their artificial microniche

The hematon-like aggregate produced could be used as an artificial microniche for a stem cell. Having shown that multilayered 3-D aggregates of different cell types could be produced, and that the aggregates could be maintained over an extended period of time, in the next set of experiments it was explored whether it was possible to introduce individual or small numbers of stem cells into the aggregate, and trace them.

Microniches were formed from Jurkat cells, Jurkat cells on top of AC3 stromal cells, and Jurkat cells on top of AC3 cells on top of osteoblast cells as described previously. The Jurkat, stromal and osteoblast cells were not stained. Mouse embryonic stem cells previously used in experiments on haematopoiesis (Krassowska et al. 2006) were stained with PKH26, and injected at very low concentrations- (5×10^3 cells per milliliter) into a continuous flow of D-sorbitol through the chamber immediately after the formation of an aggregate using dielectrophoresis. The cells were attracted to the aggregates by dielectrophoresis, with one to five stem

cells per aggregate. A fluorescent image of an aggregate with a single stem cell is shown in Fig. 6 demonstrating that an individual stained stem cell can be introduced into the aggregate and traced.

4 Conclusions

It has been demonstrated that hemispherical structures with distributions of cells similar to that in the hematon can be made using positive dielectrophoresis. The cells remain alive and active after their patterning and immobilisation. In addition, it has been shown it is possible to introduce individual prestained cells within an aggregate, allowing one to track the cell's further progress. Cells are tightly packed within the structure, facilitating cell-cell interaction within the aggregates as well as the establishment of gradients. The hemispherical structure produced could be used as an artificial microniche for haematopoietic stem cells, and variation of the position and type of cells within the structure could be a great assistance in the study of haematopoietic stem cell renewal, proliferation and differentiation, stem cell homing and cell migration, and the roles of the various interactions in this within the haematopoietic microenvironment. Finally, it should be emphasized that the dielectrophoretic approach works with *any* cell type, and that different 2- and 3-dimensional arrangements of cells can be created by changing the electrode shape, introducing cells at different times, or addressing different electrodes at different times (Alp et al. 2002). Thus, the approach taken could be used for the creation of a variety of artificial tissues and the study of cell microenvironments therein.

Acknowledgement We wish to thank the BBSRC for funding (project grant BB/D002850/1), the award of an ORS to A.S., and the EPSRC for a DTA award to M.L. We also wish to express our thanks to Mr. M. McGowan and Dr. J. Hatfield for the use of the SEEE clean rooms for microelectrode manufacture, Dr D. Jackson for the use of the confocal microscope, and Mrs. Sue Slack for help with cell culture. Finally, we would like to thank Dr Lesley Forrester, University of Edinburgh, for providing us with stem cells.

References

- C.A. Abboud, M.A. Lichtman, ed. by E. Beutler, M.A. Lichtman, B.S. Coller, T.J. Kipps, U. Seligsohn. *Williams Hematology*, 6th edn. (McGraw-Hill, New York, 2001), pp. 29–58
- D.R. Albrecht, G.H. Underhill, T.B. Wassermann, R.L. Sah, S.N. Bhatia, *Nat. Methods* **3**, 369–375 (2006). doi:10.1038/nmeth873
- B. Alp, G.M. Stephens, G.H. Markx, *Enzyme Microb. Technol.* **31**, 35–43 (2002). doi:10.1016/S0141-0229(02)00071-6
- B. Alp, J.S. Andrews, V.P. Mason, I.P. Thompson, R. Wolowacz, G.H. Markx, *IEEE Eng. Med. Biol.* **22**, 91–97 (2003). doi:10.1109/ MEMB.2003.1266052

- J.S. Andrews, V.P. Mason, I.P. Thompson, G.M. Stephens, G.H. Markx, J. Microbiol. Methods **64**, 96–106 (2006). doi:10.1016/j.mimet.2005.04.025
- S. Archer, T.T. Li, A.T. Evans, S.T. Britland, H. Morgan, Biochem. Biophys. Res. Commun. **257**, 687–698 (1999). doi:10.1006/bbrc.1999.0445
- S.N. Bhatia, *Microfabrication in Tissue Engineering and Bioartificial Organs* (Kluwer, Boston, 1999)
- I. Blazsek, J.L. Misset, M. Comissio, G. Mathe. Biomed. Pharmacother. **42**, 661–668 (1988)
- I. Blazsek, J.L. Misset, M. Benavides, M. Comisso, P. Ribaud, G. Mathe. Exp. Hematol. **18**, 259–265 (1990)
- I. Blazsek, B. Delmas Marsalet, S. Legras, S. Marion, D. Machover, J.L. Mis, Bone Marrow Transplant. **23**, 647–657 (1999). doi:10.1038/sj.bmt.1701616
- I. Blazsek, J. Chagraoui, B. Peault, Blood **96**, 3763–3771 (2000)
- K.J.J. Burg, T. Boland, IEEE Eng. Med. Biol. **22**(5), 84–91 (2003). doi:10.1109/EMEMB.2003.1256277
- L.M. Calvi, G.B. Adams, K.W. Welbrecht, J.M. Weber, D.P. Olseon, M.C. Knight et al., Nature **425**, 841–846 (2003). doi:10.1038/nature02040
- N. Flores-Rodriguez, G.H. Markx, J. Micromech. Microeng. **16**, 349–355 (2006). doi:10.1088/0960-1317/16/2/020
- A. Haake, J. Dual, Ultrasonics **42**, 75–80 (2004). doi:10.1016/j.ultras.2004.02.003
- A. Haake, A. Neild, G. Radziwill, J. Dual, Biotechnol. Bioeng. **92**, 8–14 (2005a). doi:10.1002/bit.20540
- A. Haake, A. Neild, D.H. Kim, J.E. Ihm, Y. Sun, J. Dual et al., Ultrasound Med. Biol. **31**, 857–864 (2005b). doi:10.1016/j.ultrasmedbio.2005.03.004
- C.T. Ho, R.Z. Lin, W.Y. Chang, H.Y. Chang, C.H. Liu, Lab Chip **6**, 724–734 (2006). doi:10.1039/b602036d
- M.P. Hughes, *Nanoelectromechanics in Engineering and Biology* (CRC, Boca Raton, 2002)
- A. Ito, Y. Takizawa, H. Honda, K.I. Hata, H. Kagami, M. Ueda et al., Tissue Eng. **10**, 833–840 (2004). doi:10.1089/1076327041348301
- T.B. Jones, *Electromechanics of Particles* (Cambridge University Press, Cambridge, 1995)
- A. Krassowska, S. Gordon-Keylock, K. Samuel, D. Gilchrist, E. Dzierzak, R. Oostendorp, J.D. Ansell et al., Exp. Cell Res. **312**, 3595–3603 (2006). doi:10.1016/j.yexcr.2006.08.001
- V.A. Liu, S.N. Bhatia, Biomed. Microdevices **4**, 257–266 (2002). doi:10.1023/A:1020932105236
- V.P. Mason, G.H. Markx, I.P. Thompson, J.S. Andrews, M. Manefield, FEMS Microbiol. Lett. **244**, 121–127 (2005). doi:10.1016/j.femsle.2005.01.031
- A. Menachery, R. Pethig, I.E.E. Proc. Nanobiotechnol. **152**, 145–149 (2005). doi:10.1049/ip-nbt:20050010
- V. Mironov, T. Boland, T. Trusk, G. Forgacs, R.R. Markwald, Trends Biotechnol. **21**, 157–161 (2003). doi:10.1016/S0167-7799(03)00033-7
- H. Morgan, N.G. Green, *AC Electrokinetics: Colloids and Nanoparticles* (Research Studies, Baldock, 2001)
- D.J. Odde, M.J. Renn, Biotechnol. Bioeng. **67**, 312–318 (2000). doi:10.1002/(SICI)1097-0290(20000205)67:3<312::AID-BIT7>3.0.CO;2-F
- A. Sebastian, A.M. Buckle, G.H. Markx, J. Micromech. Microeng. **16**, 1769–1777 (2006). doi:10.1088/0960-1317/16/9/003
- A. Sebastian, A.M. Buckle, G.H. Markx, Biotechnol. Bioeng. **98**, 694–700 (2007). doi:10.1002/bit.21416
- T. Shimizu, M. Yamato, A. Kikuchi, T. Okano, Biomaterials **24**, 2309–2316 (2003). doi:10.1016/S0142-9612(03)00110-8
- W. Tan, T.A. Desai, Biomaterials **25**, 1355–1364 (2004). doi:10.1016/j.biomaterials.2003.08.021
- V.L. Tsang, S.N. Bhatia, Adv. Drug Deliv. Rev. **56**, 1635–1647 (2004). doi:10.1016/j.addr.2004.05.001
- A.G. Venkatesh, G.H. Markx, J. Phys. D: Appl. Phys. **40**, 106–113 (2006). doi:10.1088/0022-3727/40/1/S15
- C.E. Verduzco-Luque, B. Alp, G.M. Stephens, G.H. Markx, Biotechnol. Bioeng. **83**, 34–44 (2003). doi:10.1002/bit.10646
- F.M. Watt, B.L.M. Hogan, Science **287**, 1427–1430 (2000). doi:10.1126/science.287.5457.1427
- L.I. Zon LI (ed.), *Hematopoiesis, A Developmental Approach* (Oxford University Press, Oxford, 2001)